Non-zonal Approaches for Grey Area Mitigation

C. Mockett, M. Fuchs, F. Thiele, S. Wallin, S.H. Peng, S. Deck, J.C. Kok, H. van der Ven, A. Garbaruk, M. Shur, M. Strelets and A. Travin

1 Introduction

The term non-zonal approach is applied in Go4Hybrid to refer to hybrid RANS-LES methods in which the model, not the user, defines the regions in which RANS and LES modes are active. Such methods are inherently more applicable to complex geometries than embedded approaches, however they are more susceptible to the grey area problem.

C. Mockett (✉) · M. Fuchs · F. Thiele
CFD Software Entwicklungs- und Forschungsgesellschaft mbH (CFDB), Bismarckstr. 10-12, 10625 Berlin, Germany
e-mail: charles.mockett@cfd-berlin.com

S. Wallin · S.H. Peng
Unit of Aeronautical and Autonomous Systems, Swedish Defence Research Agency, FOI, 16490 Stockholm, Sweden

S. Deck
ONERA, The French Aerospace Lab, 92190 Meudon, France
e-mail: sebastien.deck@onera.fr

J.C. Kok · H. van der Ven
Netherlands Aerospace Centre NLR, Anthony Fokkerweg 2, 1059 Amsterdam, CM, Netherlands

A. Garbaruk · M. Shur · M. Strelets · A. Travin
New Technologies and Services (NTS), 5A, Krasnogo Kursanta Street, 197198 St.-Petersburg, Russia

A. Garbaruk · M. Shur · M. Strelets · A. Travin
St.-Petersburg Polytechnic University, 29, Polytechnicheskaya Street, 195258 St.-Petersburg, Russia

C. Mockett et al. (eds.), *Go4Hybrid: Grey Area Mitigation for Hybrid RANS-LES Methods*, Notes on Numerical Fluid Mechanics and Multidisciplinary Design 134, DOI 10.1007/978-3-319-52995-0_2

This chapter describes the various approaches for grey area mitigation proposed by the relevant partners for non-zonal hybrid approaches. As far as possible, detailed descriptions are provided to encourage the implementation of the approaches in different codes.

All methods have in common the aim to destabilise the early separated shear layer. Some methods apply stochastic forcing to this end, whereas others seek to reduce the damping influence of eddy viscosity here. An important secondary goal has been to develop approaches that are as far as possible generally applicable and suitable for the simulation of complex geometries.

The grey area mitigation (GAM) strategies are as far as possible decoupled from the underlying hybrid RANS-LES method. Ideally, this would mean that the GAM enhancements can be applied as a retro-fit to any existing non-zonal hybrid RANS-LES approach, however various complications may limit the extent to which this is achievable in practice.

Each of the following subsections describes the methods proposed by each Go4Hybrid partner active in the relevant Task 2.1. Where applicable, references to existing publications of the methods are also listed.

2 Application of Alternative SGS Forms for Grey Area Mitigation

2.1 Rationale

A novel approach (Mockett et al. 2015) is formulated to improve the behaviour of DES in the region where an attached boundary layer (handled with RANS) flows into a separated shear layer (to be resolved using LES). The approach aims to be generally-applicable and retain the non-zonal nature of DES. Furthermore, the formulation is local and can be readily implemented in general-purpose solvers. The approach incorporates alternative SGS model formulations that discern between quasi 2D and developed 3D flow states. The modification leads to a strong reduction of eddy viscosity in the early shear layer and consequently a significant acceleration of RANS to LES transition (RLT).

Additionally, this approach can be combined with the $\tilde{\Delta}_{\omega}$ vorticity-adaptive grid scale proposal of NTS, see Sect. 6 (Alternative, Shear Layer Adapted, Subgrid Length-Scale for Non-Zonal Hybrid RANS-LES Methods), and comprehensive testing (Fuchs et al. 2014, 2015) of both formulations in isolation and in combination has been carried out by CFDB, as is reported in later chapters.

2.2 Formulation

For convenience we adopt a generalised notation for the LES models considered. For DES models in LES mode, the following form can be derived under the assumption of local equilibrium (i.e. equality of the dissipation and generation terms of the underlying transport equations):

$$\nu_{sgs} = \left(C_{sgs}\Delta\right)^2 \mathcal{D}_{sgs}(u) \tag{1}$$

where different choices of C_{sgs} (the calibrated model parameter), Δ (the grid scale measure) and $\mathcal{D}_{sgs}(u)$ (a differential operator acting on the resolved velocity field) give different SGS model formulations (see e.g. Table 1).

DES is a modification to an existing RANS model whereby the model's length scale, L_{RANS} is substituted by a DES length scale. The "delayed DES" (DDES) formulation (Spalart et al. 2006) used here includes a shield function that detects attached turbulent boundary layers and aims to ensure RANS mode there, irrespective of the grid resolution. The DDES length scale is

$$L_{DDES} = L_{RANS} - f_d \max(0, L_{RANS} - L_{LES}), \text{ with } L_{LES} = \Psi C_{DES}\Delta. \tag{2}$$

C_{DES} is a model parameter analogous to the Smagorinsky constant and Ψ is a term designed to compensate for unwanted activity of low-Re terms in LES mode (Spalart et al. 2006). Both these terms as well as the RANS length scale depend on the underlying RANS model. For the Spalart–Allmaras (SA) model (Spalart and Allmaras 1994), L_{RANS} is given by the wall-normal distance d_w, $C_{DES} \approx 0.65$ has been calibrated for decaying isostropic turbulence and the low-Re correction term is given by

$$\Psi^2 = \min\left\{10^2, \frac{1 - \frac{C_{b1}}{C_{w1}\kappa^2 f_w^*}\left[f_{t2} + (1 - f_{t2})f_{v2}\right]}{f_{v1}\max(10^{-10}, 1 - f_{t2})}\right\},$$

with $\kappa = 0.41$, $f_w^* = 0.4241$ and other parameters as defined by the SA model.

Table 1 Summary of model formulations in LES mode

Model	C_{sgs}	$\mathcal{D}_{sgs}(u)$
Smagorinsky	C_S	$\sqrt{2S_{ij}S_{ij}}$
WALE	C_W	S_W^*
σ	C_σ	S_σ^*
DES	$\sqrt{A}C_{DES}\Psi$	S_{RANS}^*
WALE-DES	$\sqrt{A}C_{DES}\Psi$	$B_W S_W^*$
σ-DES	$\sqrt{A}C_{DES}\Psi$	$B_\sigma S_\sigma^*$

For definitions of S_W^* and S_σ^* see Eqs. (4) and (6), respectively. Coefficient A depends on the underlying RANS model and may or may not be constant

The DDES shield function f_d is formulated as

$$f_d = 1 - \tanh\left[\left(C_{d1} r_d\right)^{C_{d2}}\right],$$
$$r_d = \frac{\nu_t + \nu}{\kappa^2 d_w^2 \max\left(\sqrt{\frac{\partial U_i}{\partial x_j}\frac{\partial U_i}{\partial x_j}}, 10^{-10}\right)}, \tag{3}$$

which is close to 0 inside the boundary layer and blends rapidly to 1 near the boundary layer edge. Furthermore, in free shear flows $f_d = 1$ leading to $L_{DDES} = L_{LES}$. For standard SA-DDES, the values $C_{d1} = 8$ and $C_{d2} = 3$ were proposed Nicoud et al. (2011).

As mentioned, DES can be mapped to a Smagorinsky model form in LES mode, for which several well-established shortcomings are known. Of greatest relevance here is the Smagorinsky model's inability to correctly handle laminar-to-turbulent transition, where its sensitivity to mean flow shear gives rise to high levels of eddy viscosity that attenuate the (resolved) transition process. Turning to DES, the same mechanism contributes to the RLT problem, hampering the development of resolved turbulence arising from the natural shear layer instability.

Several models without this shortcoming have been formulated by the LES research community, however many of these (e.g. dynamic and high-pass filtered models) involve non-local terms that are impractical for industrial CFD solvers.

The WALE (Nicoud et al. 1999) and σ (Nicoud et al. 2011) models—proposed by Nicoud and co-workers—however seem particularly promising for further consideration. In these approaches local velocity gradient information is processed to distinguish between essentially two-dimensional situations such as plane shear, for which very low eddy viscosity is generated, and three-dimensional turbulence, where regular SGS model activity is recovered. This should offer a highly effective measure for accelerating RANS to LES transition whilst maintaining a practical and robust local formulation. Note that our goal in adopting the WALE and σ approaches in the LES mode of DES is exclusively targeted at such RLT improvement—the use of these models in a DES framework renders issues regarding their near-wall behaviour irrelevant, since the RANS branch of DES is active there.

The key changes relative to the Smagorinsky model involve the differential operator acting on the velocity field ($\mathcal{D}_{sgs}(u)$ in Eq. (1). For the WALE model, this term is defined as

$$\mathcal{D}_{sgs}(u) = S_W^* = \frac{\left(\mathcal{S}_{ij}^d \mathcal{S}_{ij}^d\right)^{3/2}}{\left(S_{ij} S_{ij}\right)^{5/2} + \left(\mathcal{S}_{ij}^d \mathcal{S}_{ij}^d\right)^{5/4}}, \tag{4}$$

where $S_{ij} = 1/2\left(\partial U_i/\partial x_j + \partial U_j/\partial x_i\right)$ and $\mathcal{S}_{ij}^d$ is the traceless symmetric part of the square of the velocity gradient tensor

$$\begin{aligned} \mathcal{S}_{ij}^{d} &= \frac{1}{2}\left(g_{ij}^{2} + g_{ji}^{2}\right) - \frac{1}{3} g_{kk}^{2} \delta_{ij}, \\ g_{ij}^{2} &= g_{ik} g_{kj}, \\ g_{ij} &= \frac{\partial U_i}{\partial x_j}. \end{aligned} \tag{5}$$

For the σ model, the corresponding definition is

$$\mathcal{D}_{sgs}(u) = S_{\sigma}^{*} = \frac{\sigma_3(\sigma_1 - \sigma_2)(\sigma_2 - \sigma_3)}{\sigma_1^2}, \tag{6}$$

where $\sigma_1 \geq \sigma_2 \geq \sigma_3 \geq 0$ are the three singular values of the velocity gradient tensor $\boldsymbol{g} = g_{ij}$. We chose the second method proposed by Nicoud et al. (2011) to compute these, since it is self-contained and involves negligible computational overhead.

Although derived with very different considerations, both the WALE and σ models return very low values of SGS viscosity in plane shear flows and involve negligible computational overhead. The analysis in Nicoud et al. (2011) however indicates that the σ model possesses greater generality. Both approaches were tested for a range of complex flows, from which a preference for the σ emerged; although returning similar results for flows approximating planar shear, the σ formulation performed far superior to WALE for the more complex delta wing flow topology (Fuchs et al. 2015), see in see in Part IV: Chapter "Delta Wing at High Angle of Attack".

To modify DES to behave like the WALE and σ models in LES mode, we leave the length scale substitution unmodified (Eq. 2) and introduce an additional function to substitute the corresponding term for $\mathcal{D}_{sgs}(u)$ in the LES mode region only. The velocity gradient invariant in the underlying RANS model, S_{RANS}^{*}[1] is substituted by

$$S_{(W,\sigma)-DDES}^{*} = S_{RANS}^{*} - f_d \mathrm{pos}(L_{RANS} - L_{LES})\left(S_{RANS}^{*} - B_{W,\sigma} S_{W,\sigma}^{*}\right), \tag{7}$$

where the operator used to detect DES97 RANS and LES mode acts as

$$\mathrm{pos}(a) = \begin{cases} 0 & \text{if } a \leq 0 \\ 1 & \text{if } a > 0 \end{cases}.$$

Where the DDES shield function f_d is active, the values are blended smoothly according to the value of f_d. As such, the blending occurs at the same location as the length scale blending of DDES. Note that if the grid is sufficiently coarse that the interface between RANS and LES would occur outside the boundary layer (according to DES97), Eq. (7) gives a discontinuous switch between S_{RANS}^{*} on the RANS side and $B_{W,\sigma} S_{W,\sigma}^{*}$ on the LES side of the interface. On the other hand, if we

[1]For the SA model, $S_{RANS}^{*} = \sqrt{2\Omega_{ij}\Omega_{ij}}$ is substituted (not $\tilde{S}$).

would not apply the discontinuous pos-function in Eq. (7), the LES mode of the $S^*_{(W,\sigma)-DDES}$ term would be activated as soon as f_d deviates from zero, which would not be desirable considering the coarseness of the grid.

It was found that the f_d function needed recalibrating for the WALE and σ DDES variants, since the rapid drop in $S^*_{(W,\sigma)-DDES}$ near the boundary layer edge caused thinning of the shielded region. For SA-based WALE-DDES and σ-DDES, setting the value of $C_{d1} = 10$ in Eq. (3) was found to restore equivalent blending to standard SA-DDES. Corresponding results are shown in the following section.

For the SA model, the coefficient A is defined as

$$A_{SA} = \frac{C_{b1} f_{v1}}{C_{w1} f_w} \frac{\tilde{S}}{S^*}. \tag{8}$$

The resulting form of the model in LES mode is given in Table 1 with reference to Eq. (1). The factor $B_{W,\sigma}$ is included in $\mathcal{D}_{sgs}(u)$ such that C_{sgs} is equivalent between DES variants, since C_{DES} contributes to the RANS-LES interface determination and the pure LES models have widely different values of C_{sgs}. In principle the value of this parameter can be derived as $B_{W,\sigma} = C^2_{W,\sigma}/C^2_S$, which is checked for isotropic turbulence as shown in the next section. For a given underlying RANS model and numerical method, a single value of C_{DES} is hence maintained for all variants. The expression for Ψ is unaltered by the WALE/σ modification.

2.3 Calibration for Isotropic Turbulence

Whilst improving RLT behaviour, the proposed modifications give unchanged functionality in "fully-developed" LES turbulence. This is demonstrated using decaying isotropic turbulence, for which model and code-specific values of C_{sgs} and the coefficients B_W and B_σ have been calibrated. The arising calibrated values are listed in Table 2 and strong similarity for the turbulent spectra is seen in Fig. 1. The calibrated values are quoted only as a guideline, since recalibration for a different numerical implementation is considered essential.

2.4 Shield Function Recalibration

As mentioned previously, the boundary layer shielding function f_d needed to be recalibrated for use in conjunction with the WALE-DDES and σ-DDES variants. A flat plate boundary layer on an "ambiguous" grid (Spalart et al. 2006), i.e. one where $\Delta < \delta$ is used for this purpose. Note that this exercise has so far only been

Table 2 Values of model parameters calibrated for isotropic turbulence

Parameter	Calibrated value
C_S	0.20
C_W	0.58
C_σ	1.68
C_{DES} (for SA-DES)	0.65
B_W	8.08
B_σ	67.8

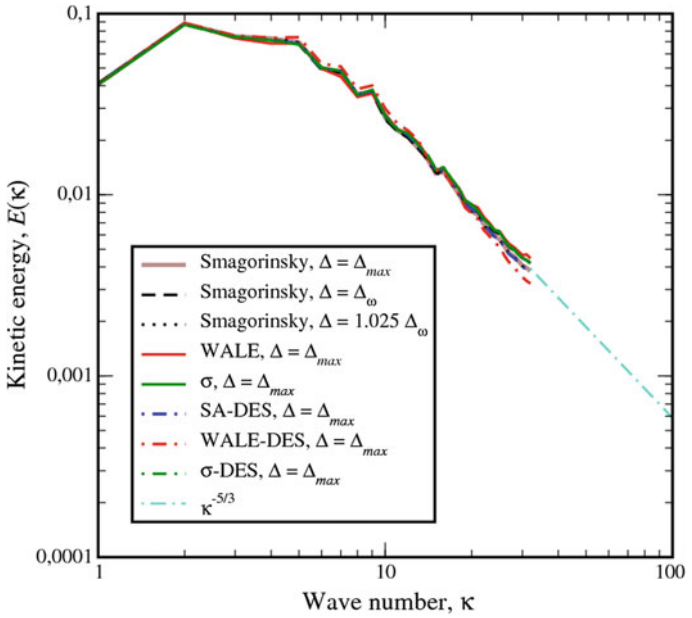

Fig. 1 Comparison of spectra for decaying isotropic turbulence obtained on a 64^3 grid from all model variants using the constant values listed in Table 1. Also shown are spectra obtained using the $\tilde{\Delta}_\omega$ grid scale definition proposed by NTS (see Sect. 5)

carried out for SA-based DDES variants and that different values could be expected to be suitable for different underlying RANS models (Gritskevich et al. 2011).

Recalibrating the shield function (Eq. 3) coefficient to $C_{d1} = 10$ whilst leaving the exponent unchanged at $C_{d2} = 3$ restores functionality equivalent to standard SA-DDES. Example plots for SA-WALE-DDES are shown in Fig. 2 (identical behaviour was seen for SA-σ-DDES).

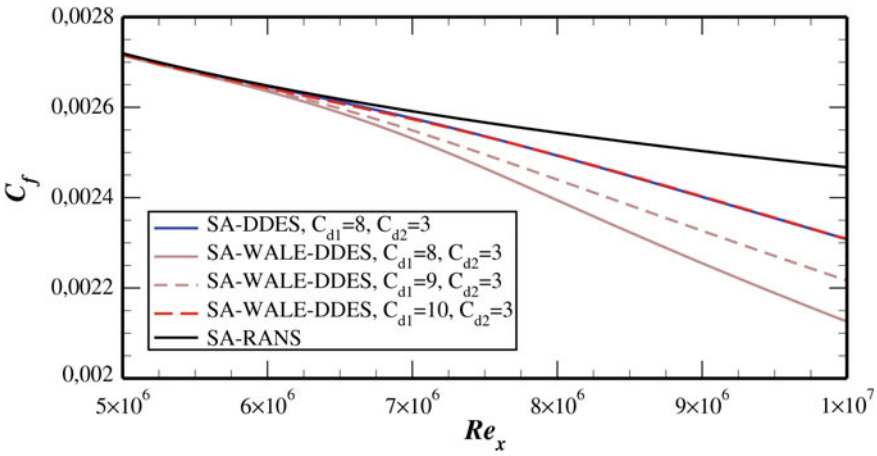

Fig. 2 Recalibration of boundary layer shielding function of SA-WALE-DDES for a flat plate on an "ambiguous" grid

3 Towards Grey-Area Mitigation Based on Different Energy Transfer Methods

3.1 Scale Energy Transfer in PANS Methods

In a computational model of turbulent flow with partly resolved turbulence the primary task for the turbulence model is to dissipate the cascaded energy at the smallest resolved scales. For an energy-consistent method where we are solving for the unresolved turbulence kinetic energy, K_u (or K_{SGS}), the dissipated energy at the resolved scales is added as a production term to the unresolved energy. The magnitude of the energy dissipation is closely related to the physical equilibrium spectral energy cascade.

In a computational model of turbulent flow with varying resolution in time and space, the additional energy transfer associated with the changing resolution must be considered, which will add new dynamics into the equations for momentum and unresolved turbulence. The additional energy transfer between resolved and unresolved scales is decoupled from the physical energy cascade and is an artefact of the computational setup.

Girimaji and Wallin (2011, 2013) derived these additional energy transfer terms in the case of varying computational resolution in the stream-wise direction. The same approach can be taken also for resolution variation in the cross-stream direction (Wallin and Girimaji 2014), which is of relevance in e.g. partly resolved boundary layer flows.

The PANS equations for the unresolved turbulence $K_u = f_k K$ when f_k is varying can be written

$$\frac{DK_u}{Dt} = P_u - \varepsilon_u + \frac{\partial}{\partial x_k}\left(v' \frac{\partial K_u}{\partial x_k}\right) + P_{Tr} + D_{Tr} \tag{9}$$

where

$$P_{Tr} = \frac{K_u}{f_k}\frac{Df_k}{Dt} \tag{10}$$

$$D_{Tr} = -\frac{K_u}{f_k}\frac{\partial}{\partial x_k}\left(\left(v + \frac{v_u}{\sigma_k'}\right)\frac{\partial f_k}{\partial x_k}\right) \tag{11}$$

are the energy scale transfer terms mainly in the stream-wise and cross-stream directions, respectively. These are directly quantified in these relations without any ad hoc modelling.

The first term, P_{Tr}, represents the transfer of turbulence energy from resolved to unresolved scales when the resolution is decreased when following the flow. That is when Df_k/Dt is positive. The opposite, increasing resolution, results in a negative P_{Tr} and a transfer of energy from unresolved to resolved scales.

The second term, D_{Tr}, represents the redistribution of turbulence energy mainly in the cross stream direction. This term will result in a flux of unresolved turbulence from regions with low f_k to regions with high f_k. Computations of partly resolved boundary layers would require that f_k decreases from 1 near the wall to some low value in the outer part of the boundary layer. The additional D_{Tr} term will then result in a sharpening of the interface region forcing unresolved turbulence in the inner part of the transition region. And, more importantly, forcing the resolved turbulence in the outer part of the transition region.

Corresponding terms in the momentum equation need to be introduced. The basic requirements on such a model are (i) the model should conserve the additional energy scale transfer and (ii) the model should interact with the mean flow at the smallest resolved scales. Different approaches can be taken including stochastic forcing and test filtering. In Wallin and Girimaji (2011) and Girimaji and Wallin (2013) the simplest possible approach was taken by introducing an energy transfer viscosity v_{Tr}. Energy conservation will dictate

$$v_{Tr} = \frac{P_{Tr} + D_{Tr}}{2S_{ij}S_{ij}},\ S_{ij} = \frac{1}{2}\left(\frac{\partial U_i}{\partial x_j} + \frac{\partial U_j}{\partial x_i}\right) \tag{12}$$

Also energy transfer to the resolved scales can be realized through a negative v_{Tr}. Usually negative viscosity is associated with unbounded exponential growth of resolved energy, but with the aid of energy conservation the growth is limited by the unresolved turbulence K_u. This was demonstrated in Girimaji and Wallin (2013).

3.2 Some Results

Decaying isotropic turbulence was computed (Girimaji and Wallin 2013) with changing resolution in time, see Fig. 3. The resolution is controlled by the PANS parameter f_k on a fixed fine grid. The energy scale transfer described above is used. The case with decreasing resolution where f_k is going from 0.3 to 0.7 is well predicted and the energy is consistently transferred from resolved to unresolved scales. Also the more difficult case with increasing resolution is at least qualitatively captured.

Channel flow at $Re_\tau = 4000$ was computed. Here, the cross-stream transfer term D_{Tr} is active. The mean velocity is not well predicted and not shown here. Figure 4 shows the shear stress split into resolved, unresolved and scale transfer. The transfer term strongly transfers energy to the unresolved scales in the outer part of the interface region. Interesting to note that the iso-surface of zero total viscosity $(= \nu + \nu_u + \nu_{Tr})$ clearly shows turbulence-like streaks with relatively small length scales without any explicit structural forcing.

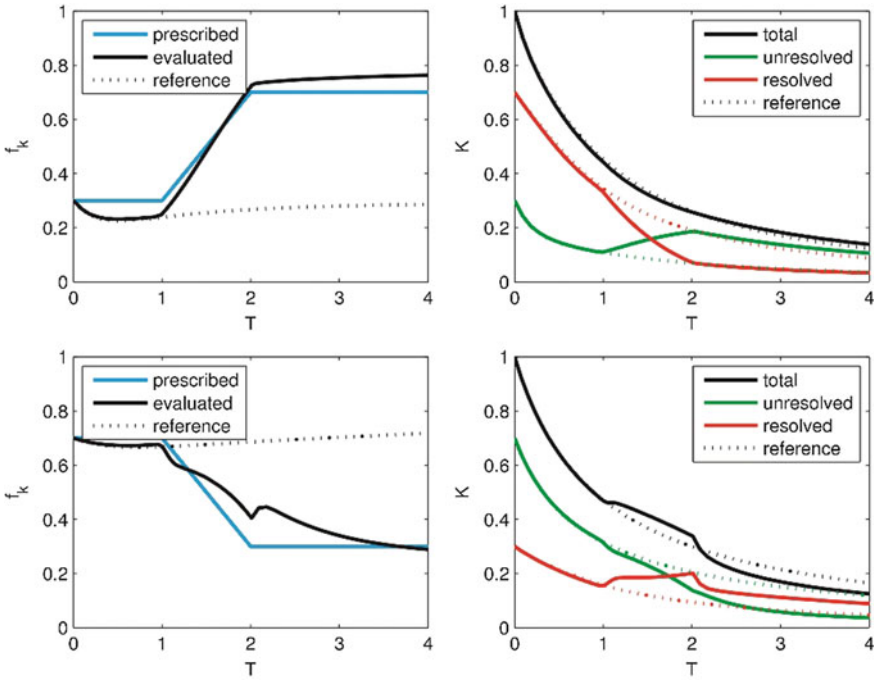

Fig. 3 Decaying isotropic turbulence with decreasing (*top*) and increasing (*bottom*) resolution with energy scale transfer active

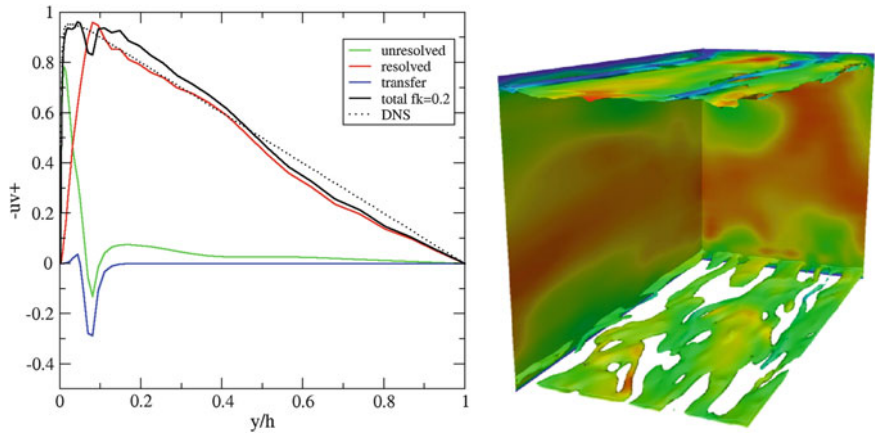

Fig. 4 Channel flow, Re = 4000, with energy scale transfer active. Shear stress (*left*) and iso-surface of zero total viscosity (*right*)

Scale Energy Transfer in Terms of ν_t

Consider the energy spectrum in Fig. 5. In the inertial range the spectrum is given by

$$E(\kappa) = C^* \varepsilon^{2/3} \kappa^{-5/3} \tag{13}$$

with the Kolmogorov constant $C^* \approx 1.5$. The physical energy transfer rate, σ, from resolved to unresolved energy, or the energy cascade, is constant within the inertial range and equals the dissipation rate ε for equilibrium turbulence. In a turbulence resolved simulation the cut-off between resolved and unresolved (sub grid) scales is given by the cut-off wave number κ_c. The energy transfer, from resolved to unresolved scales is given by σ and is represented by the SGS dissipation through the SGS viscosity, ν_{SGS}.

For simulations with variable resolution, $\kappa_c(t)$, additional energy must be transferred between resolved and unresolved scales. Let us denote this additional transfer as σ_{Tr}. In equilibrium flows (constant spectrum) this is identical to $\mathcal{P}_{Tr}$ in the PANS formulation. Now, the additional transfer can be related to the model spectrum

$$\sigma_{Tr} = -E(\kappa_c)\frac{d\kappa_c}{dt} = -C^* \left(\frac{\varepsilon}{\kappa_c}\right)^{2/3} \frac{1}{\kappa_c}\frac{d\kappa_c}{dt}. \tag{14}$$

With the filter $\Delta = \pi/\kappa_c$ one gets

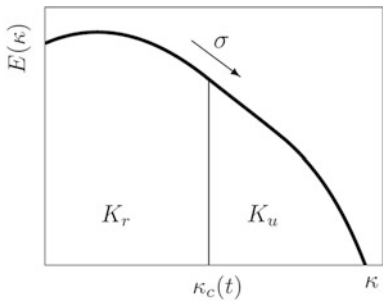

Fig. 5 Energy spectrum divided into resolved and unresolved parts (K_r and K_u) by the cut-off wave number κ_c

$$\sigma_{Tr} = \frac{C^*}{\pi^{2/3}}(\varepsilon\Delta)^{2/3}\frac{1}{\Delta}\frac{d\Delta}{dt} \tag{15}$$

Here, ε can be estimated from the SGS dissipation, $\varepsilon \approx (\nu_{SGS})S^2$, $S^2 = 2S_{ij}S_{ji}$, $S_{ij} = \left(U_{i,j} + U_{j,i}\right)/2$.

The total energy transfer rate from resolved to unresolved scales for variable resolution (VR) simulations is then given by the sum $\sigma_{VR} = \sigma + \sigma_{Tr}$. Or $\sigma_{VR} = f_{VR}\sigma$, where (with $\sigma = \varepsilon$)

$$f_{VR} = 1 + \frac{\sigma_{Tr}}{\sigma} = 1 + \frac{C^*}{\pi^{2/3}}\frac{\Delta^{2/3}}{\varepsilon^{1/3}}\frac{1}{\Delta}\frac{d\Delta}{dt} \tag{16}$$

Decreasing filter width ($d\Delta/dt < 0$) implies reduced SGS dissipation and with $f_{VR} < 0$ there is a net negative dissipation. Here, one must be clear that this is only a computational consequence that is not related to physical back scatter.

With an eddy-viscosity model for the SGS stresses the SGS dissipation is given by $\varepsilon \approx \nu_{SGS}S^2$. The variable resolution is considered simply by replacing SGS viscosity by $\nu_{VR} = f_{VR}\nu_{SGS}$.

In the expression for f_{VR}, the derivative is evaluated as the advection by the resolved flow

$$\frac{1}{\Delta}\frac{d\Delta}{dt} = \frac{d\ln(\Delta)}{dt} = \left(\frac{\partial \ln(\Delta)}{\partial t} + U_k\frac{\partial \ln(\Delta)}{\partial x_k}\right). \tag{17}$$

The estimate of the SGS dissipation, or ε, might be cumbersome with insufficient resolution and numerical dissipation. At least the molecular viscosity should be added to ν_{SGS} so that $\varepsilon \approx (\nu + \nu_{SGS})S^2$ but better approximations might be needed. The term $\Delta^{2/3}/\varepsilon^{1/3}$ is the time scale of the unresolved turbulence and can be expanded to (using $\nu_{SGS} = (C_s\Delta)^2 S$, with $C_S = 0.12$)

$$\frac{\Delta^{2/3}}{\varepsilon^{1/3}} \approx \left(\frac{\Delta^2}{(\nu + \nu_{SGS})S^2}\right)^{\frac{1}{3}} = \left(\frac{\Delta^2}{\left(\nu + C_s^2\Delta^2 S\right)S^2}\right)^{\frac{1}{3}} \approx \frac{1}{C_s^{2/3}S} \tag{18}$$

For avoiding division by zero when $S \to 0$ we will limit S by some fraction of a viscous time scale, $\max(S, c_1 v/\Delta)$.

The final expression for the variable-resolution correction then becomes

$$f_{VR}(\Delta) = 1 + \frac{C_{VR}}{\max(S, c_1 v/\Delta)} \left(\frac{\partial \ln(\Delta)}{\partial t} + U_k \frac{\partial \ln(\Delta)}{\partial x_k} \right) \tag{19}$$

where

$$C_{VR} = \frac{C^*}{\pi^{2/3} C_s^{2/3}} \approx 2.9 \tag{20}$$

Negative f_{VR} would lead to negative v_{SGS}. With $v_{VR} < -v$ the total viscosity becomes negative and the computation might become numerically unstable. Such situation can only be permitted when the computational back scatter is connected with a transport equation for the SGS energy. If not, f_{VR} should be limited to 0, or possible slightly negative values. Also a similar upper limit should apply, maybe $f_{VR} < 2$.

Limiting f_{VR} will effectively pile up the rate of change of the filter width. Hence, the limiting of f_{VR} must be accomplished with diminishing rate of change of the filter width. Since the flow is transported by the velocity field, the filter width must be governed by a transport equation. The equation is derived from the following assumptions.

First, let $g_0 = \ln(\Delta_0)$, where Δ_0 is the filter width from the present hybrid method. Then, let $g = \ln(\Delta)$ be the modified filter with the implicit requirement that $|f_{VR}(\Delta) - 1| < 1$. Following a stream line

$$f_{VR}(t) = 1 + C \frac{\mathrm{d}g(t)}{\mathrm{d}t} \tag{21}$$

where $C = C_{VR}/\max\left(S, c_1 v/\Delta^2\right)$. Moreover, an equation for $g(t)$ could be

$$\frac{\mathrm{d}g(t)}{\mathrm{d}t} = c'(g_0(t) - g(t)) \tag{22}$$

Hence, $g(t)$ is driven towards $g_0(t)$. The limitation of $f_{VR}(\Delta)$ (or $|f_{VR} - 1| < C_{FLim}$), where C_{FLim} might be slightly different than unity, can be implied as

$$\left| C \frac{\mathrm{d}g}{\mathrm{d}t} \right| = \left| Cc'(g_0 - g) \right| < C_{FL} \tag{23}$$

or

$$c^{'} = \frac{1}{C}\min\left(c_0^{'}, \frac{C_{FL}}{|g_0 - g|}\right) \tag{24}$$

which gives

$$\begin{aligned} \frac{\mathrm{d}g}{\mathrm{d}t} &= \frac{1}{C}\min\left(c_0^{'}, \frac{C_{FLim}}{|g_0 - g|}\right)(g_0 - g) \\ f_{VR} &= 1 + \min\left(c_0^{'}, \frac{C_{FLim}}{|g_0 - g|}\right)(g_0 - g) \\ \nu_{VR} &= f_{VR}\nu_{SGS} \end{aligned} \tag{25}$$

where the energy-transfer corrected viscosity ν_{VR} replaces the ordinary SGS viscosity ν_{SGS}.

The behaviour of $g = \ln(\Delta)$ following the transport equation is illustrated in Fig. 6 for a situation that mimics the mixing layer. The green curve (g_0) corresponds to a typical hybrid length scale that falls from a RANS level for $x < 0$ to a LES level with slightly increasing grid size in the downstream direction until $x \approx 1$ where the grid is coarsened. The red curve is the corresponding solution of the transport equation for g that is relaxed towards the g_0 value. The rate of change is clearly visible and is illustrated by f (or actually $f - 1$ in this plot) where the magnitude of the rate of change is limited to 1. Hence, the SGS viscosity with the energy transfer correction, ν_{Tr}, will be effectively close to zero for $x \lesssim 0.3$.

Extending to a PDE (compressible flow) gives

$$\frac{\partial \rho \mathrm{g}}{\partial t} + U_k\frac{\partial \rho \mathrm{g}}{\partial x_k} = \frac{\rho}{C}\min\left(c_0^{'}, \frac{C_{FLim}}{|g_0 - g|}\right)(g_0 - g) + \frac{\partial}{\partial x_k}\left(\left(\mu + \frac{\mu_t}{\sigma_g}\right)\frac{\partial \mathrm{g}}{\partial x_k}\right) \tag{26}$$

where $C = C_{VR}/\max\left(S, c_1\nu/\Delta_0^2\right)$ and the coupling to the baseline model is concluded here.

- $g_0 = \ln(\Delta_0)$ is given by the length scale of the baseline model (Δ in the LES region and $\Delta_{RANS} = l_{RANS}/C_s$ in the RANS region).
- The RANS viscosity is unchanged and the corrected viscosity in the LES region is given by

$$\nu_{VR} = f_{VR}\nu_{SGS}, f_{VR} = 1 + \min\left(c_0^{'}, \frac{C_{FLim}}{|g_0 - g|}\right)(g_0 - g) \tag{27}$$

- where $C_{VR} = 2.9$, $c_1 = 10$, $c_0^{'} = 2.0$, $\sigma_g = 0.1$, $C_{FLim} = 1.0$.

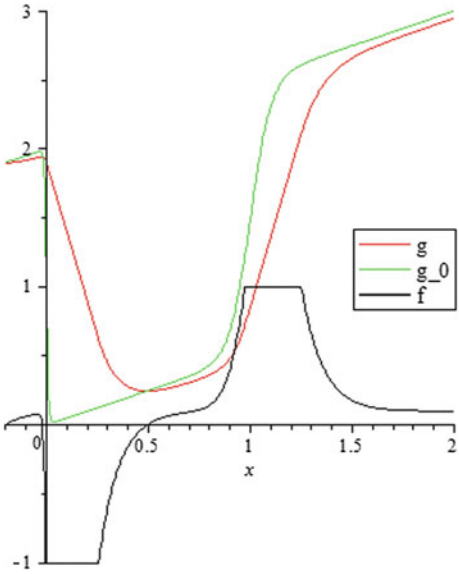

Fig. 6 Solution of $g(x)$ for a case similar to the mixing layer with fixed $U_C = 0.2$, $c_0^{'} = 2$ and $c_1 = 10$

3.3 *Peng HYB0 with Energy Transfer Correction*

The next step is to implement the f_{VR} corrected SGS viscosity for a hybrid model and we choose Peng HYB0 model to start with. Peng HYB0 model is given here in a slightly different form. The RANS length scale is $\tilde{l}_\mu = f_\mu \kappa d$, where $\kappa = 0.418$ and d is the wall distance. The wall damping function is $f_\mu = \tanh(R_t^{1/3}/2.5)$ where $R_t = \tilde{\mu}/\mu$, $\tilde{\mu} = \rho \tilde{l}_\mu^2 S$, $S^2 = 2S_{ij}S_{ji}$ and $S_{ij} = \left(U_{i,j} + U_{j,i}\right)/2$. $f_\mu = 1$ away from walls.

The LES length scale is $l_{SGS} = C_s \Delta$ where $C_s = 0.12$ and $\Delta = \sqrt{\left(\Delta_{\max}^2 + \Delta_{\text{vol}}^2\right)/2}$, $\Delta_{\max} = \max\left(\Delta_x, \Delta_y, \Delta_z\right)$ and $\Delta_{\text{vol}} = \delta V^{1/3}$.

The modified RANS length scale considering interface matching is $l_\mu = f_s \tilde{l}_\mu$ where

$$f_s = \frac{1}{2}\left(e^{-\frac{R_s^{0.75}}{4.75}} + e^{-\frac{R_s^{0.3}}{2.5}}\right), R_s = \left(\tilde{l}_\mu / l_{SGS}\right)^2 \tag{28}$$

The hybrid length scale now becomes

$$l_h = \begin{cases} l_\mu, \tilde{l}_\mu < \Delta \\ l_{SGS}, \tilde{l}_\mu \geq \Delta \end{cases} \tag{29}$$

and the hybrid viscosity $\mu_h = \rho l_h^2 S$.

The energy transfer extension is implemented as following:

1. The equation for g follows Eq. (26).
2. The driving filter width $\Delta_0 \rightarrow g_0$ is given by $\Delta_0 = \tilde{l}_\mu / C_s$ in RANS or $\Delta_0 = \Delta$ in LES.
3. Inflow B.C. for g is $g_\infty = \ln\left(v_{T,\infty}/\sqrt{K_\infty}\right)$. Wall B.C. is $g_{wall} = -20$ (corresponds to $\Delta \rightarrow 0$).
4. The SGS viscosity is modified according to Eq. (27). The RANS viscosity is kept unchanged.
5. The tentative values for the model coefficients are:
   - $\sigma_g = 0.1$ for high smoothing of g
   - $C^* = 1.5$
   - $c_0^{'} = 2.0$
   - $C_{FLim} = 1.0$

For the first test computations $C^* = 5.0$ was used to exaggerate the effect and $C_{Flim} = 0.8$ for avoiding effective viscosities too close to zero.

3.4 DDES with Energy Transfer Correction

The idea is to apply the energy transfer correction in the same way as for the HYB0 model above. In addition to the v_T equation (or the K–ω equations), the equation for g is applied.

The energy transfer extension is implemented as following:

1. The equation for g follows Eq. (26).
2. The driving filter width $\Delta_0 \rightarrow g_0$ is given by $\Delta_0 = l_{RANS}/C_s$ in RANS or $\Delta_0 = \Delta$ in LES.
3. Inflow B.C. for g is $g_\infty = \ln\left(v_{T,\infty}/\sqrt{K_\infty}\right)$. Wall B.C. is $g_{wall} = -20$ (corresponds to $\Delta \rightarrow 0$).
4. The SGS viscosity is modified according to Eq. (27). The RANS viscosity is kept unchanged.
5. The model coefficients are:
   - $\sigma_g = 0.1$ for high smoothing of g
   - $C^* = 1.5$
   - $c_0^{'} = 2.0$
   - $C_{FLim} = 1.0$ or slightly lower

3.5 Energy-Backscatter Function Incorporated in the LES Mode

The so-called "grey-area" problem in hybrid RANS-LES modelling is closely associated to the RANS-LES interface, being usually reflected by a delayed re-establishment of resolved turbulence in the LES region neighboring immediately to the RANS region. To improve the prediction, one may either improve the fed-in turbulence contents from RANS to LES via the interface or enhance the turbulence-resolving capabilities of the LES mode. Apart from the PANS-based method described previously, another method to examine is further introduced, which invokes the energy-backscatter function in the SGS model formulation to enhance turbulence-resolving capability in the LES region. This means that the SGS model is of mixed type that is able to induce instantaneous reverse energy transfer from the SGS to the resolved large-scale turbulence, in conjunction with the conventional energy dissipation based on the SGS eddy-viscosity formulation. The theoretical analysis and derivation of the SGS modelling formulation was reported previously by Peng and Davidson (2001) applying the Leonard expansion (Peng and Davidson 2009) to the SGS residual stress tensor. The SGS stress tensor has been modelled in a two-term formulation (Peng 2012), namely,

$$\tau_{ij} \approx \underbrace{(C_L f_L \Delta)^2 \frac{\partial \bar{u}_i}{\partial x_k}\frac{\partial \bar{u}_j}{\partial x_k}}_{\text{Leonard Term}, L_{ij}} - \underbrace{2 f_D v_{sgs} \bar{S}_{ij}}_{\text{Second Term}} \tag{30}$$

The first term is the Leonard term, which is similar to a similarity SGS model and plays a role in backscattering turbulent energy from SGS to large-scale turbulence, and the second term is the conventional part for energy dissipation based on SGS eddy viscosity. The SGS viscosity in the second term is determined in the form of the Smagorinsky model or cast in a formulation of one-equation SGS model based on the SGS turbulent kinetic energy k_{sgs}. In previous work for modelling calibration, v_{sgs} has been modelled with the Smagorinsky model.

The capability of LES with the two-term SGS model has been well demonstrated for turbulent channel flow (Peng 2012), as shown in Fig. 7 as an example in computation for turbulent channel flow at $Re_\tau = 550$.

Note that the Leonard term can be viewed as the leading term in the reconstruction series of the conventional similarity model with double-filtered residuals according to Peng and Davidson (2001). In Fig. 8a the modelled turbulent shear stress by the Leonard term is illustrated in comparison with that by the Smagorinsky term. In Fig. 8b, the energy-backscatter function due to the Leonard term is further analyzed. The energy transfer has been approximated with $\varepsilon = -\tau_{ij} S_{ij}$. It is shown that the Leonard term has induced about (15–20)% reverse energy transfer of the total. In general, the two-term SGS model (of mixed type) has shown an overall reasonable performance. The LES mode is then incorporated into hybrid RANS-LES modelling.

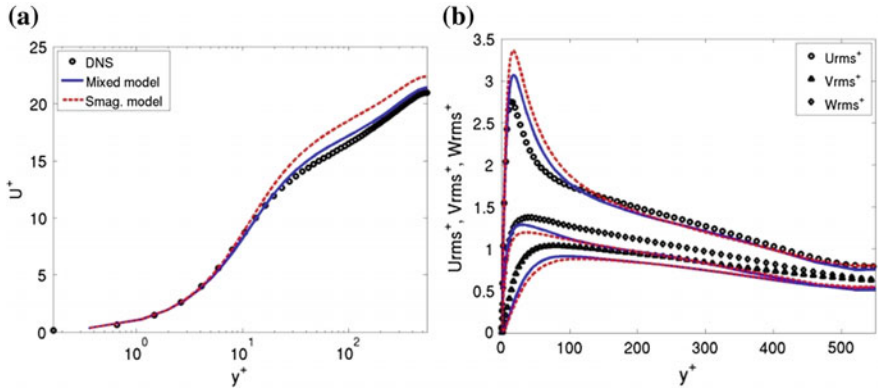

Fig. 7 LES with the two-term algebraic SGS model for turbulent channel flow ($Re_\tau = 550$), in comparison the Smagorinsky model. **a** Mean streamwise velocity; **b** Resolved velocity fluctuations

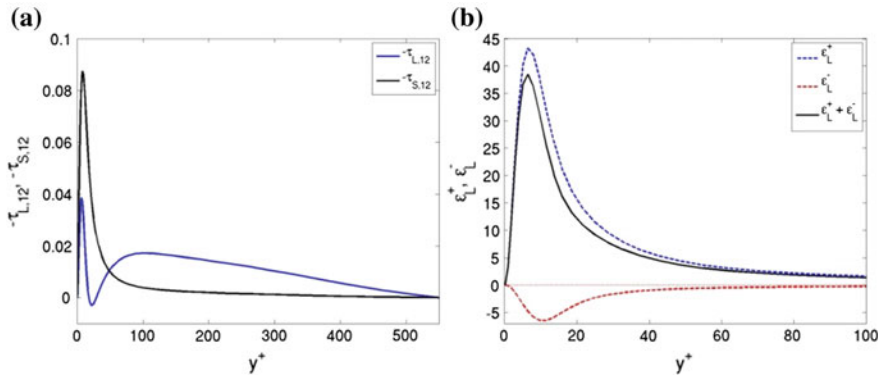

Fig. 8 LES with the two-term algebraic SGS model for turbulent channel flow $Re_\tau = 550$. **a** Modelled turbulent shear stress for the Leonard term and the Smagorinsky term; **b** Modelled energy transfer due to the Leonard term

3.6 Algebraic Hybrid RANS-LES Formulation (HYB0M Model)

With appropriate calibration and validation, the SGS model of mixed-type given in the above equation can be used as the LES mode in hybrid RANS-LES formulation, in which the function of energy-backscatter can be exploited to enhance the LES-resolved large-scale turbulent fluctuations. In the FOI work, an algebraic hybrid RANS-LES model (HYB0) according to Peng (2005, 2006) has been taken as the baseline model, where the Smagorinsky-type model has been used for energy dissipation in the LES mode. Using the HYB0 formulation as the platform for testing, the two-term SGS model is then incorporated in the hybridized LES mode,

in which the energy-backscatter term is expected to support a more effective re-establishment of resolved turbulent fluctuations. After entering into the LES region immediately after the RANS-LES interface, this may to some extent mitigate so-called "grey area" problem. In conjunction with the Smagorinsky model, the SGS mixed model takes the form of

$$\tau_{ij} = \tau_{L,ij} + \tau_{S,ij} = (C_L\Delta)^2 f_L \frac{\partial \bar{U}_i}{\partial x_k}\frac{\partial \bar{U}_j}{\partial x_k} - 2f_D(C_S\Delta)^2|\bar{S}|\overline{S_{ij}} \tag{31}$$

where $f_L = \tanh(R_{sgs})$, $f_D = f_w \tanh(R_{sgs}/5)$ with $f_w = 1 - e^{y^+/10}$, $R_{sgs} = \nu_{sgs}/\nu$, $C_S = 0.12$ and $C_L = \sqrt{1/12}$.

For the hybrid RANS-LES modelling formulation, note that the Leonard term plays only a role in the LES mode. This term is thus shielded in the near-wall RANS region by introducing a "shielding" function, f_b, which complies with $f_b = 0$ for the RANS mode and $f_b = 1.0$ in the LES region. This has led to a formulation for the hybrid RANS-LES model, which reads

$$\tau_{ij} \approx -2\mu_h\overline{S_{ij}} + (C_L f_L \Delta)^2 f_b \frac{\partial \bar{u}_i}{\partial x_k}\frac{\partial \bar{u}_j}{\partial x_k} \tag{32}$$

The hybrid eddy viscosity, μ_h, takes the same formulation as given by the baseline HYB0 model (Peng 2005, 2006). The shielding function is defined in terms of the ratio of the RANS length scale, $\tilde{l}_\mu$, and the SGS length scale, Δ, namely, $f_b = tanh\left[(R_l/2)^8\right]$ with $R_l = \tilde{l}_\mu/\Delta$. The resulting model is termed the HYB0M model and the details of the modelling formulation can be found in Peng (2012).

The HYB0M model has been validated and verified in computations of 2D turbulent hill flow and for the flow over a backward-facing step (Peng 2012). As shown respectively in Fig. 9 (for 2D hill flow) and Fig. 10 (for the backward-facing step flow), the incorporation of the energy-backscatter function in the LES mode has induced some improvement in the prediction, having slightly enhanced the resolved turbulent energy. The formulation has been further verified and improved in computations of test cases defined in the project.

For better numerical treatment of the Leonard term, the energy-backscatter method has been formulated by introducing an effective eddy viscosity, ν^*. Equation (32) is written as

$$\tau_{ij} = (C_L f_L \Delta)^2 f_b \frac{\partial \bar{u}_i}{\partial x_k}\frac{\partial \bar{u}_j}{\partial x_k} - 2\nu_h S_{ij} = L_{ij} - 2\nu_h S_{ij} \tag{33}$$

In Eq. (33), the first term on the right-hand side is the Leonard term, which may induce instantaneous energy backscatter. In the computation it was found that this term may trigger numerical instabilities when the instantaneous reverse energy transfer becomes large. This term needs thus t be limited. For an improved

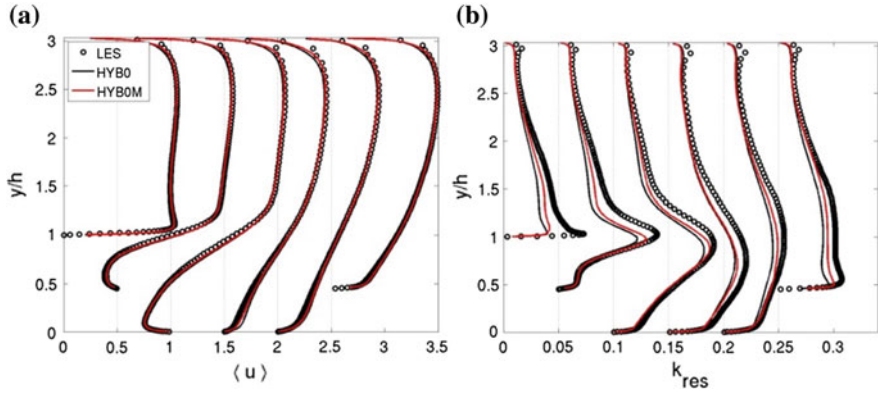

Fig. 9 HYB0 M computation for turbulent 2D periodic hill flow, in comparison the baseline HYB0 model. **a** Mean streamwise velocity; **b** Resolved turbulent kinetic energy

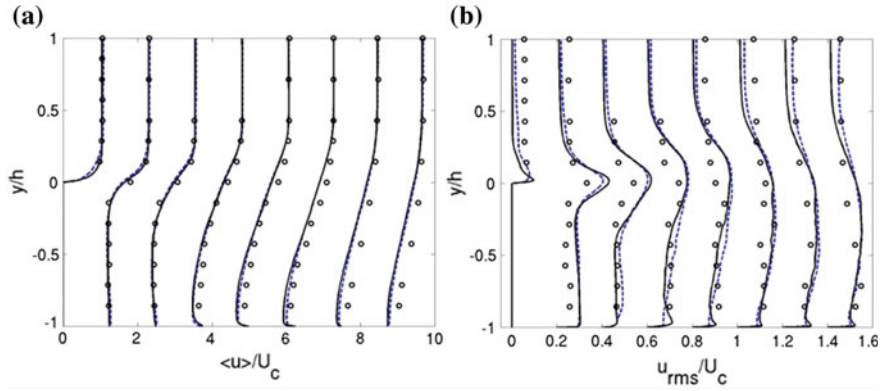

Fig. 10 HYB0 M computation (*solid line*) for turbulent backward-facing step flow in comparison the baseline HYB0 model (*dashed line*). **a** Mean streamwise velocity; **b** Resolved turbulent fluctuations of streamwise velocity

numerical treatment, the Leonard term is split into two parts, viz. $L_{ij} = L^*_{ij} + L^d_{ij}$, where L^*_{ij} is assumed to be responsible for the energy transfer and L^d_{ij} is the deviatoric part. The first part, L^*_{ij}, is modelled using an effective eddy viscosity in terms of $L^*_{ij} = -2\nu^* S_{ij}$. Using S_{ij} to contract L_{ij}, and let $L^d_{ij} S_{ij} = 0$, ν^* can then be computed by

$$\nu^* = -\frac{L_{ij} S_{ij}}{2 S_{ij} S_{ij}} \tag{34}$$

L_{ij}^{d} is then computed by $L_{ij}^{d} = L_{ij} - L_{ij}^{*}$. With this formulation in the HYB0M computations, a negative value of v^{*} is limited by $v^{*} \geq -(v_h + v)$ for numerical stability. This may to some extent have restricted the GAM function. In conjunction with HYB1 model, this is much alleviated, however, since the Leonard term enters also into the production term of the k-equation. Being incorporated in the HYB0 model (resulting the HYB0M model), it has been verified that a redefinition of the SGS turbulence length scale in the HYB0 model can further alleviate the grey-area problem. This is done by replacing the maximum local cell size, δ_{max}, with the minimum one, δ_{min}, namely, in the definition of Δ,

$$\Delta = \sqrt{\left(\delta_{min}^{2} + \delta V^{2/3}\right)/2} \tag{35}$$

where δ_{min} has been used to replace δ_{max} used in the original definition. With this definition of Δ, both the HYB0 and HYB0M models have shown sensible improvement for mitigating the grey area in the initial stage of the mixing layer, for example.

4 Overview of Zonal Detached Eddy Simulation (ZDES) and Grid Scale Definitions for Modes I and II

4.1 Formulation

The Zonal DES (ZDES) approach was first proposed by Deck (2005a, b) and the complete formulation has been recently published in Deck (2012). The method is based on a fluid problem-dependent zonalisation and makes possible the use of various formulations within the same calculation.

In the framework of ZDES, three specific hybrid length scale formulations [see Eq. (36)], also called modes, are optimized to be employed on three typical flow field topologies as illustrated in Fig. 11. Though the method can be adapted to any turbulence model, in the framework of the underlying SA model (Spalart and Allmaras 1994), d_w is replaced with $\tilde{d}_{ZDES}$ in the model according to:

$$\tilde{d}_{ZDES} = \begin{cases} d_w & \text{if } mode = 0 \text{ (i.e. RANS)} \\ \tilde{d}_{DES}^{I} & \text{if } mode = 1 \\ \tilde{d}_{DES}^{II} & \text{if } mode = 2 \\ \tilde{d}_{DES}^{III} & \text{if } mode = 3 \end{cases} . \tag{36}$$

Mode 1 concerns flows where the separation is triggered by a relatively abrupt variation in the geometry; mode 2 is retained when the location of separation is induced by a pressure gradient on a gently curved surface, and mode 3 for flows

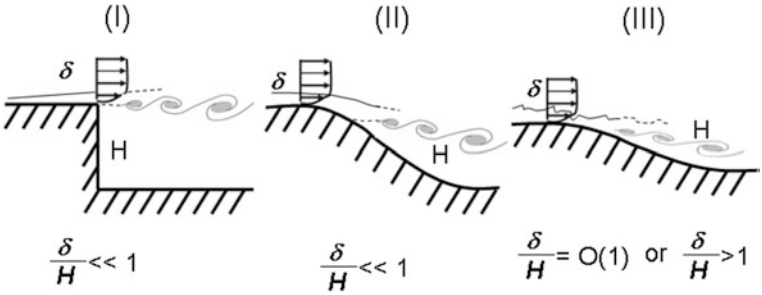

Fig. 11 Classification of typical flow problems. *I* separation fixed by the geometry, *II* separation induced by a pressure gradient on a gently-curved surface, *III* separation strongly influenced by the dynamics of the incoming boundary layer

where the separation is strongly influenced by the dynamics of the incoming boundary layer (see Fig. 11). All these flow cases may be treated by the same ZDES technique in its different modes. An example where the three modes of ZDES are used at the same time on a curvilinear geometry can be found in Deck (2013).

In practice, the formulas of ZDES differ from those of DES97 or DDES in the definition of the ZDES length scale, the subgrid length scale and the treatment of the near wall functions in the LES mode as detailed in the following.

- Mode I of ZDES (*mode* = 1), location of separation fixed by the geometry

$$\tilde{d}^{I}_{DES} = \min\left(d_w, C_{DES}\tilde{\Delta}^{I}_{DES}\right) \tag{37}$$

- Mode II of ZDES (*mode* = 2), location of separation unknown a priori:

$$\tilde{d}^{II}_{DES} = d_w - f_d \max\left(0, d_w - C_{DES}\tilde{\Delta}^{II}_{DES}\right) \tag{38}$$

- Mode III of ZDES (*mode* = 3), Wall-Modelled LES (WMLES):

$$\tilde{d}^{III}_{DES} = \begin{cases} d_w & \text{if } d < d_w^{interface} \\ \tilde{d}^{I}_{DES} & \text{otherwise} \end{cases} \tag{39}$$

It is important to note that with mode 2 of ZDES, which clearly borrows ideas from DDES (Spalart et al. 2006), it is permitted to operate in an "automatic" manner since $\tilde{d}^{II}_{DES}$ employs the same protection function as DDES to maintain the RANS behaviour in the attached boundary layer. The improvement lies in the definition of the subgrid length scale $\tilde{\Delta}$ as will be discussed in the following.

Concerning this latter mode devoted to WMLES (described in detail in Part II (Chapter "Improved Embedded Approaches", Sect. 4: ZDES mode 3), the switching into LES mode occurs at a given altitude $d_w^{interface}$ prescribed by the user. In this mode (see Deck et al. 2014; Chauvet et al. 2007), the solution has to be fed with turbulent inflow content.

A second important ingredient of ZDES is the definition of the subgrid length scale $\tilde{\Delta}$ entering Eqs. (37), (38) and (39). Indeed, analogous to the classical LES exercise $\tilde{\Delta}$ controls which wavelengths can be resolved as well as the eddy viscosity levels. Though physically justified in the frame of DES97/DDES (Spalart et al. 2006) aimed to shield the attached boundary layer from MSD, the slow delay in the formation of instabilities in free shear layers of DDES has been partly attributed to the use of the maximum grid extension $\Delta_{\max} = \max(\Delta x, \Delta y, \Delta z)$ as subgrid length scale. The use of the time-honoured cube root of the cell volume $\Delta_{\text{vol}} = (\Delta x\ \Delta y\ \Delta z)^{1/3}$ decreases dramatically the level of predicted eddy viscosity because this latter value is proportional to the square of the filter width. Chauvet et al. (2007) proposed an efficient flow-dependent definition based on the orientation of the vorticity vector $\vec{\omega}$ aimed at solving the slow LES development in mixing layers. A generalization of Chauvet et al. subgrid length scale has been proposed by Deck (2012) (especially for unstructured grids) and may read as:

$$\Delta_\omega = \sqrt{\bar{S}_\omega} \tag{40}$$

where $\bar{S}_\omega$ is the average cross section of the cell normal to $\vec{\omega}$. More precisely; it introduces the notion that at any spatiotemporal point, if the vorticity is not zero, there exists one particular direction indicated by the vorticity $\vec{\omega}$ (Fig. 12).

The subgrid length scale that enters Eqs. (37) and (38) is respectively given by:

$$\tilde{\Delta}_{DES}^{I}\left(\Delta x, \Delta y, \Delta z, U_{i,j}\right) = \Delta_{vol} \text{ and } \Delta_\omega \tag{41}$$

and

$$\tilde{\Delta}_{DES}^{II} = \begin{cases} \Delta_{max} & \text{if } f_d \leq f_{d0} \\ \Delta_{vol} \text{or} \Delta_\omega & \text{if } f > f_{d0} \end{cases} \tag{42}$$

$\tilde{\Delta}_{DES}^{II}$ clearly borrows ideas from DDES in the sense that the f_d sensor is employed to determine whether $\Delta_{\max}$ or Δ_{vol} (or Δ_ω) is used. Equations (41) and (42) are not a minor adjustment in the DES framework since the modified $\tilde{\Delta}$ length scales depend not only on the grid but also on the velocity and eddy viscosity fields. It is important to emphasize that the shielding of the boundary layer is still ensured

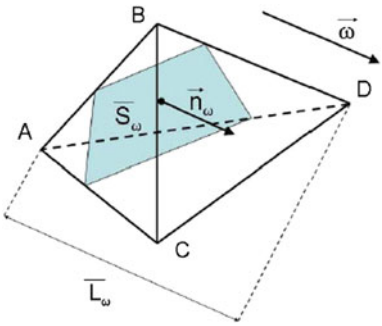

Fig. 12 Definition of the subgrid length scale $\Delta_\omega = \sqrt{\bar{S}_\omega}$. $\bar{S}_\omega$ is the average cross section of the cell normal to the vorticity vector $\vec{\omega}$

by the function f_d which behaves as standard DDES ($\Delta = \Delta_{max}$) as long as $f_d < f_{d0}$. The improvement lies in Δ_ω (or Δ_{vol}) becoming the new subgrid length scale when $f_d > f_{d0}$ which solves the delay in the formation of instabilities (see Deck 2012).

5 NLR Approaches to Grey-Area Mitigation for Non-zonal Methods

5.1 Introduction

Two types of approaches are proposed to mitigate the grey-area issue for non-zonal DES methods, in particular the X-LES method:

- Triggering instabilities by introducing a stochastic subgrid-scale (SGS) model.
- Reducing the level of SGS stresses in initial shear layers, caused by high gradients of the mean velocity.

For both types, the baseline methods previously incorporated in X-LES, and used with some success to improve the capturing of free shear layers, are described below as well as a new method that has been investigated within the Go4Hybrid project. The baseline methods consist of a stochastic eddy-viscosity model (Kok and van der Ven 2009) and a high-pass filtered SGS model (Kok and van der Ven 2012), respectively. The new method incorporates a stochastic backscatter model (Kok 2016). Note that the approaches described can also be applied to other non-zonal DES methods.

5.2 The X-LES Method

In non-zonal DES methods such as X-LES (Kok et al. 2004), a single set of turbulence-model equations is used to model both the Reynolds stresses in RANS zones and the subgrid-scale (SGS) stresses in LES zones. An eddy-viscosity model is used for these stresses, which are then given by the Boussinesq hypothesis:

$$\tau_{ij} = 2\nu_t\left(S_{ij} - \frac{1}{3}\partial_k u_k \delta_{ij}\right) - \frac{2}{3}k\delta_{ij},$$

with ν_t the eddy viscosity, $S_{ij} = \frac{1}{2}\left(\partial_j u_i + \partial_i u_j\right)$ the rate-of-strain tensor, and k the turbulent or subgrid-scale kinetic energy.

The X-LES method in particular is based on the TNT k–ω model. The method switches to LES when the RANS length scale $\left(l = \sqrt{k}/\omega\right)$ exceeds the LES length scale ($C_1\Delta$, with Δ the filter width and $C_1 = 0.08$). The RANS length scale is then replaced by the LES length scale in the expression for the eddy viscosity as well as in the expression for the dissipation of turbulent kinetic energy ε:

$$\nu_t = \min\{l, C_1\Delta\}\sqrt{k},$$

and

$$\varepsilon = \frac{\beta k^{3/2}}{\min\{l, C_1\Delta\}},$$

with $\beta = 0.09$. The filter width Δ is defined at each grid point as the maximum of the mesh width in all directions. Note that effectively a k-equation SGS model is used in LES zones (where $l > C_1\Delta$), as ω drops out of the expressions for ν_t and ε.

5.3 Stochastic SGS Models

The current baseline stochastic eddy-viscosity SGS model (Kok and van der Ven 2009) attempts to destabilize shear layers by introducing a stochastic variable ξ in the expression for the eddy viscosity in LES mode. The stochastic variable has a standard normal distribution with zero mean and unit variance: $\xi = N(0, 1)$. For the X-LES method, the expression for the eddy viscosity then becomes:

$$\nu_t = \begin{cases} k/\omega, & \text{if } l \le C_1\Delta, \\ \xi^2 C_1\Delta\sqrt{k}, & \text{if } l > C_1\Delta. \end{cases}$$

At each time step, a new, uncorrelated value of ξ is drawn for every grid cell. The stochastic term is not included in the expression for the turbulent dissipation ε.

This stochastic eddy-viscosity model was not aimed at modelling energy backscatter. Furthermore, when this model is combined with the high-pass filtered SGS models of the next section, then its effect is diminished due to (much) lower values of the rate-of-strain tensor.

As an alternative approach, a new stochastic SGS model (Kok 2016) is considered that models backscatter at the theoretically correct rate. It is based on the models of Leith (1990) and Schumann (1995). Its formulation is presented in detail here, but a more extensive explanation is given by Kok (2016). The subgrid stress tensor is defined as

$$\tau_{ij} = 2\nu_t\left(S_{ij} - \frac{1}{3}\partial_k u_k \delta_{ij}\right) - \frac{2}{3}k\delta_{ij} - R_{ij},$$

with R_{ij} a random stress tensor that is responsible for the backscatter. This tensor is not modelled directly, but, following Leith, its gradient is modelled as the rotation of a stochastic vector potential:

$$\nabla \cdot \boldsymbol{R} = \nabla \times (C_B k \boldsymbol{\xi}),$$

with C_B a model constant ($C_B = 1$ by default) and $\boldsymbol{\xi}$ a vector of three independent stochastic variables $\xi_i = N(0,1)$. The stochastic variables are assumed to be uncorrelated in space over distances larger than the filter width Δ and uncorrelated in time over time intervals larger than the subgrid time scale $\tau \sim \Delta/\sqrt{k}$.

The additional stochastic term $\nabla \cdot \boldsymbol{R}$ is effectively a random acceleration that is added to the momentum equation. As it is solenoidal, it does not induce pressure fluctuations and therefore will not function as a noise source.

Note that the value of k in the initial shear layer will be high if the upstream boundary layer is turbulent, whereas it will be practically zero if the upstream boundary layer is laminar. In the former case, the stochastic model may destabilize the shear layer, whereas in the latter case the stochastic model will be effectively switched off, allowing a natural laminar-to-turbulent transition of the shear layer.

An essential modification that has been investigated for the stochastic backscatter model is to include non-zero spatial and temporal correlations of the stochastic variables ξ_i. These correlations are obtained by solving stochastic differential equations that are defined below, leading essentially to the following correlations of ξ_i—see Kok (2016) for more details:

$$\mathrm{E}\left(\xi_i(\boldsymbol{x},t)\xi_j(\boldsymbol{y},s)\right) = \delta_{ij} e^{-d^2/2} \mathrm{e}^{|t-s|/\tau},$$

with $d^2 = \|\boldsymbol{x}-\boldsymbol{y}\|^2/\left(C_\Delta \Delta^2\right)$ and $\tau = C_\tau \Delta/\sqrt{k}$. For the model to be Galilean invariant, this correlation should be interpreted in Lagrangian sense, i.e., $\boldsymbol{x}$ and $\boldsymbol{y}$ are the time-dependent coordinates of fluid particles. The default values for the model constants are $C_\Delta = 0.1$ and $C_\tau = 0.05$.

To obtain temporal correlations, a stochastic Langevin-type differential equation is solved for each component ξ_i, given by

$$\rho\xi_i dt + \tau\left(\frac{\partial\rho\xi_i}{\partial t} + \nabla\cdot(\rho\boldsymbol{u}\xi_i)\right)dt = \sqrt{2\tau}\rho dW_i,$$

with $\mathrm{d}W_i(\boldsymbol{x},t)$ the differential of a Wiener process $W_i(\boldsymbol{x},t)$ with the properties

$$\mathrm{d}W_i(\boldsymbol{x},t) = \mathrm{N}(0,\mathrm{d}t)$$

and

$$\mathrm{E}\big(\mathrm{d}W_i(\boldsymbol{x},t)dW_j(\boldsymbol{y},s)\big) = \delta_{ij}e^{-d^2/2}\delta(t-s)\mathrm{d}t\mathrm{d}s.$$

This equation is discretized with second-order central schemes both in space and time (second-order finite-volume in space and mid-point rule in time):

$$(\rho\boldsymbol{\xi})^n_{i,j,k} + \frac{\tau}{\delta t}\left((\rho\boldsymbol{\xi})^{n+1/2}_{i,j,k} - (\rho\boldsymbol{\xi})^{n-1/2}_{i,j,k}\right) + \tau\nabla_{i,j,k}\cdot((\rho\boldsymbol{u})^n\boldsymbol{\xi}^n) = \sqrt{2\tau/\delta t}\rho^n_{i,j,k}\boldsymbol{\eta}^n_{i,j,k},$$

with $f^n = \frac{1}{2}\left(f^{n+1/2} + f^{n-1/2}\right)$, δt the time step, n the time-step index, (i,j,k) the grid-cell indices, and $\nabla_{i,j,k}$ the second-order central finite-volume discretization of the gradient operator. Thus, at each time step n, first a new value of the stochastic variable $\boldsymbol{\eta}^n_{i,j,k}$ must be determined and then a new value of the stochastic variable $\boldsymbol{\xi}^n_{i,j,k}$ can be determined by solving the equation above. The stochastic variable $\boldsymbol{\eta}^n_{i,j,k}$ should be uncorrelated in time and should have, at each grid cell, three independent components with zero mean, unit variance, and spatial correlation $\exp(-d^2/2)$.

Note that the stochastic variable $\boldsymbol{\xi}$ is a 3-component vector and therefore three temporal equations need to be solved. This can be done simultaneously with the main flow and turbulence-model equations. These three equations are solved in the complete flow domain, with $\boldsymbol{\eta}^n_{i,j,k} = 0$ in the RANS zones and at all external boundaries.

The variable $\boldsymbol{\eta}^n_{i,j,k}$ can be obtained by applying a spatial smoother to a stochastic variable $\boldsymbol{\zeta}^n_{i,j,k} = N(0,1)$ that is drawn independently at each grid cell (i,j,k) and at each time step n. To obtain the desired spatial correlation of $\boldsymbol{\eta}^n_{i,j,k}$ on a structured grid, three implicit smoothing operators per computational direction are applied to the spatially uncorrelated variable $\boldsymbol{\zeta}^n_{i,j,k}$:

$$\left(I - \beta_i\delta_i^2\right)\left(I - \beta_j\delta_j^2\right)\left(I - \beta_k\delta_k^2\right)\boldsymbol{\eta}'_{i,j,k} = \boldsymbol{\zeta}^n_{i,j,k},$$

with I the identity operator, $\beta_i = C_\Delta(\Delta/\delta_i x)^2$ the smoothing coefficient in i-direction, $\delta_i x$ the mesh size in i-direction, and δ_i^2 the second-order difference operator in i-direction. To ensure a unit variance, the smoothed variable is scaled as

$$\boldsymbol{\eta}^{n}_{i,j,k} = \frac{(1+4\beta_i)^{3/4}\left(1+4\beta_j\right)^{3/4}(1+4\beta_k)^{3/4}}{(1+2\beta_i)^{1/2}\left(1+2\beta_j\right)^{1/2}(1+2\beta_k)^{1/2}}\boldsymbol{\eta}^{'}_{i,j,k}.$$

The implicit smoothing requires solving a tridiagonal system per computational direction, which can be done efficiently using the Thomas algorithm. At the boundaries, Dirichlet boundary conditions ($\boldsymbol{\eta}' = 0$) are applied.

5.4 High-Pass Filtered SGS Models

As shear layers are initially very thin, they contain high gradients of the (mean) velocity, and therefore of the rate of strain, which leads to high values of the subgrid stresses. Any instability of the initial shear layer may then be damped by these high stresses, thus delaying the development of resolved turbulence. The approach to grey-area mitigation considered in this section attempts to reduce these high values of the stresses.

A high-pass filtered (HPF) SGS model (Kok and van der Ven 2012) has been included in X-LES to remove the dependency of the stresses on (high) mean velocity gradients. The SGS stresses are computed from the velocity fluctuations u' instead of the instantaneous velocity u:

$$\tau_{ij} = 2\nu_t\left(S^{'}_{ij} - \frac{1}{3}\partial_k u^{'}_k \delta_{ij}\right) - \frac{2}{3}k\delta_{ij}, \text{ if } \quad l > C_1\Delta,$$

with $S_{ij} = \frac{1}{2}\left(\partial_j u'_i + \partial_i u'_j\right)$. The velocity fluctuations u' are obtained by applying a temporal high-pass filter to the velocity field. This high-pass filter consists of subtracting the running time average of the velocity from the instantaneous velocity:

$$u^{'}(x,t) = u(x,t) - \bar{u}(x,t),$$

with the running time average given by

$$\bar{u}(x,t) = \frac{1}{t}\int_0^t u(x,s)\mathrm{d}s,$$

which is discretized as (dropping dependency on x)

$$\bar{u}(t_n) = \frac{n-1}{n}\bar{u}(t_{n-1}) + \frac{1}{n}u(t_n).$$

A possible disadvantage of this particular high-pass filter is that the running time average contains the complete time history, with equal weight, including the transient. In practice, however, this does not appear to lead to a significant slow-down of the statistical convergence or to a lengthening of the transient.

The baseline high-pass filter is less suitable when the flow contains some non-turbulent unsteadiness at a low frequency that should also be filtered out.

Alternatively, high-pass filters that filter out all frequencies below a certain cut-off frequency may be considered to overcome this disadvantage. In order to limit memory requirements, time-discrete (or digital) filters that can be computed recursively may be chosen, such as the Butterworth-type filters. A disadvantage of these filters is that the cut-off frequency must be chosen a priori. The cut-off frequency should be lower than the frequency of the smallest resolved turbulent structures and higher than the frequency of any non-turbulent unsteadiness. For the test cases considered in Go4Hybrid, which do not contain any non-turbulent unsteadiness, the baseline high-pass filter was found to be sufficient.

6 Alternative, Shear Layer Adapted, Subgrid Length-Scale for Non-zonal Hybrid RANS-LES Methods

6.1 Introduction

A new definition of the subgrid length scale is proposed, which aims at a rapid destabilising the separated shear layers and accelerating RANS-to-LES transition within non-zonal RANS-LES hybrid methods. In a sense, the proposed approach which underlying physics is outlined in detail in a recent publication of Shur et al. (2015), is similar to that of CFDB (see Sect. 2, above), since both approaches take advantage of the peculiarities of the flow and/or grid topology in the early shear layers. However, implementation of this idea in the two approaches is quite different: the CFDB approach relies upon an alternative SGS model formulation that discerns between quasi 2D and developed 3D flow states, whereas NTS uses for this purpose an alternative subgrid length-scale definition. This definition includes two ingredients, both involving specially designed kinematic criteria accounting for the abovementioned peculiarities of the early shear regions. Although so far this definition has been applied only with the Delayed DES (DDES) approach (Spalart et al. 2006), it is expected to be transferrable to any non-zonal hybrid RANS-LES method employing the grid scale as the LES filter width definition and to pure LES models as well. Below we outline both ingredients of the proposed definition and present its final formulation.

6.2 Formulation of Vorticity-Adaptive Grid Scale Measure

In the following, we consider, e.g., jet shear layers or trailing edges and define x, y and z to be aligned with the streamwise direction, across the shear layer, and in the spanwise or azimuthal direction, respectively. In such situations, efficient grids are fine in the y direction and perhaps also in x, but coarse in z. This creates "pencil" or "ribbon" grid cells. The maximum cell size definition of Δ normally used with DES is

$$\Delta_{\max} = \max(\Delta_x, \Delta_y, \Delta_z). \tag{43}$$

Although this is a rational and robust choice for archetypal LES in the inertial range with near-cubic cells, it turns out to be too "conservative" in the initial region of shear layers resolved by such anisotropic grids.

Chauvet et al. (2007) introduced the promising concept of sensitising Δ to the orientation of the vorticity vector with the grid. The formulation was subsequently generalised for unstructured meshes by Deck (2012). In regions where the flow is essentially 2D with the vorticity axis aligned with the coarse z direction, their Δ_ω quantity reduces to $\sqrt{\Delta_x \Delta_y}$, thus removing the dominance of Δ_z. Although this is helpful, we consider the strong influence of the smallest grid direction in this formulation troublesome. This is the same as our objection to the commonplace use of the cubic root of the cell volume, which was introduced by Deardorff (1970) without logical justification. We therefore propose an alternative concept that reduces to $\max(\Delta_x, \Delta_y)$.

Considering a cell with its centre at r and vertices at $\mathbf{r}_n (n = 1, \ldots, 8$ for hexahedra), the proposed definition reads as:

$$\tilde{\Delta}_\omega = \frac{1}{\sqrt{3}} \max_{n,m=1,8} |(\mathbf{I}_n - \mathbf{I}_m)|, \tag{44}$$

where $\mathbf{l}_n = \mathbf{n}_{\boldsymbol{\omega}} \times (\mathbf{r}_n - \mathbf{r})$ and $\mathbf{n}_{\boldsymbol{\omega}}$ is the unit vector aligned with the vorticity vector. Thus, the quantity $\tilde{\Delta}_\omega$ is the diameter of the set of cross-product points l_n divided by $\sqrt{3}$.

As intended, in the shear layer situations outlined above it reduces to $\frac{1}{\sqrt{3}} \left(\Delta_x^2 + \Delta_y^2 \right)^{1/2}$, i.e. is $O\left(\max\left\{\Delta_x, \Delta_y\right\}\right)$. In 3D cases, $\tilde{\Delta}_\omega$ is of the order of $\Delta_{\max}$ except for the situation when the vorticity vector is aligned with one of the grid coordinate directions (e.g., k), when it reduces to $O\left(\max\left\{\Delta_i, \Delta_j\right\}\right)$. Therefore, the smallest grid-spacing never rules.

Another improvement over the original proposal (Chauvet 2007; Deck 2012) occurs when the shear layer is skewed so that the vortex cores are not aligned with the z direction. In such a case, the Kelvin–Helmholtz instability cannot be resolved well, yet the original definition does not recognise this situation rapidly enough and keeps Δ excessively small.

Testing for isotropic turbulence on an isotropic grid has shown that $\tilde{\Delta}_\omega$ indeed adopts on average 97.5% of the value of Δ_{max}. To balance this, $\tilde{\Delta}_\omega$ can be multiplied by a factor 1.025. The influence of this is however very minor.

6.3 Testing for Backward-Facing Step

In order to evaluate a performance of the length-scale and $\tilde{\Delta}_\omega$ versus the conventional DES length-scale Δ_{max}, DDES has been conducted of the flow over a backward-facing step with the use of both length-scales. The grid resolution in the homogeneous spanwise direction has furthermore been varied between $\Delta_z/H = 0.1$ and $\Delta_z/H = 0.05$, where H is the step height.

The grid used in the simulations and visualisation of the activity of the $\tilde{\Delta}_\omega$ quantity are shown in Fig. 13a, b, respectively. In the very early shear layer, where

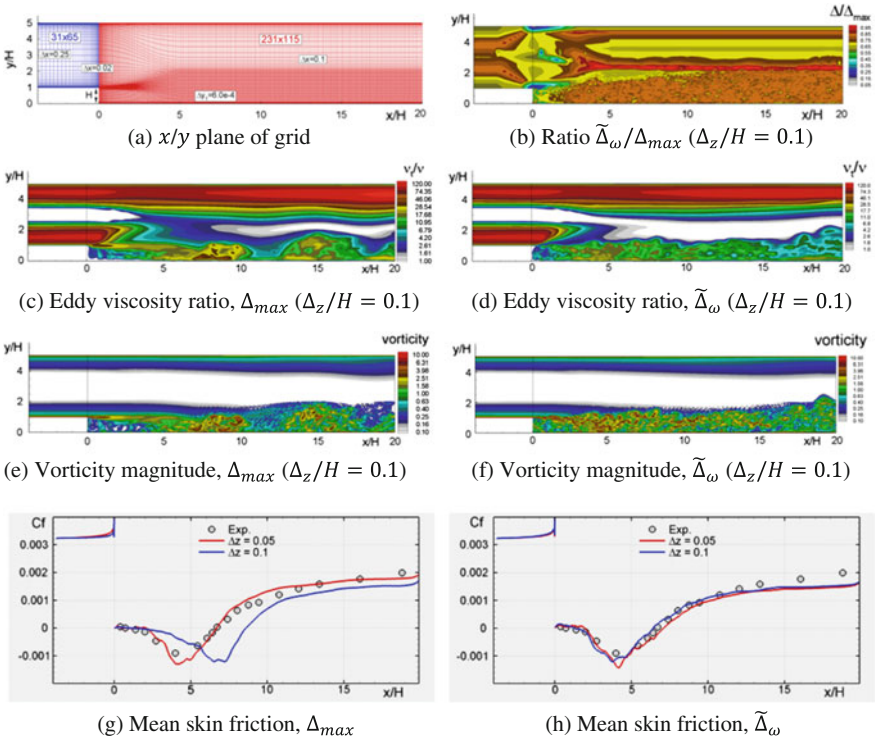

(a) x/y plane of grid

(b) Ratio $\tilde{\Delta}_\omega/\Delta_{max}$ ($\Delta_z/H = 0.1$)

(c) Eddy viscosity ratio, Δ_{max} ($\Delta_z/H = 0.1$)

(d) Eddy viscosity ratio, $\tilde{\Delta}_\omega$ ($\Delta_z/H = 0.1$)

(e) Vorticity magnitude, Δ_{max} ($\Delta_z/H = 0.1$)

(f) Vorticity magnitude, $\tilde{\Delta}_\omega$ ($\Delta_z/H = 0.1$)

(g) Mean skin friction, Δ_{max}

(h) Mean skin friction, $\tilde{\Delta}_\omega$

Fig. 13 Visualisation and results for SA-DDES comparing the Δ_{max} and $\tilde{\Delta}_\omega$ grid scale measures for backward-facing step flow; experimental data of Vogel and Eaton (1985)

the grid cells are highly anisotropic and the vorticity vector is aligned with the z direction, $\tilde{\Delta}_\omega$ gives significantly reduced values relative to Δ_{max}. Further downstream, where three-dimensional resolved turbulence has developed, values of between around 70 and 85% of Δ_{max} are seen. Correspondingly, eddy viscosity levels (Fig. 13c, d) are strongly reduced in the early shear layer, enabling a significantly accelerated development of resolved structures (Fig. 13e, f). Note also, that owing to the DDES shield function, the eddy viscosity levels in the attached boundary layers (treated with RANS) are unaffected, as intended.

As seen from the distributions of mean skin friction coefficient on the lower wall (Fig. 13g, h), the agreement with experiment is improved significantly by the $\tilde{\Delta}_\omega$ formulation for the coarser $\Delta_z/H = 0.1$ mesh. Furthermore, the strong sensitivity of the Δ_{max} results to the spanwise mesh resolution is dramatically reduced using the $\tilde{\Delta}_\omega$ expression, which is a highly desirable result.

6.4 *Extension of Formulation with "Vortex Tilting Measure" (VTM)*

On a nearly isotropic (cubic) grid the effect of replacing Δ_{max} with $\tilde{\Delta}_\omega$ is marginal. So, provided that the isotropic grid is not sufficiently fine to ensure a proper resolution of the initial nearly-2D region of a shear layer,[2] one needs an additional, purely kinematic, measure allowing the identification of quasi-2D flow regions in which nearly Implicit LES treatment is desirable for facilitating the Kelvin-Helmholtz instability and accelerating transition to developed turbulence.

Such a measure called Vortex Tilting Measure (VTM) has been proposed. The measure presents a normalized upper bound of the cross product of the vortex-changing term $S_{ij}\omega_j$ and the vorticity vector ω_i and reads as:

$$\mathrm{VTM} \equiv \frac{\sqrt{6}\left|(\hat{\mathbf{S}}\cdot\boldsymbol{\omega})\times\boldsymbol{\omega}\right|}{\omega^2\sqrt{3tr(\hat{\mathbf{S}}^{\mathbf{2}})-[tr(\hat{\mathbf{S}})]^2}} \tag{45}$$

where $\hat{\mathbf{S}}$ is the strain tensor, $\boldsymbol{\omega}$ is the vorticity vector and $tr(\cdot)$ means trace.

Thus defined measure varies in the range [0, 1.0], is small (close to zero) in the quasi-2D flow regions (where the vorticity vector is an eigenvector of the strain tensor), and mostly close to 1.0 in the developed 3D turbulence.

With the use of the VTM quantity, the length-scale $\tilde{\Delta}_\omega$ (Spalart et al. 2006) may be further modified as:

[2]Note that this is the case in all practically meaningful simulations, since "fine enough" actually means unaffordable.

$$\Delta_{SLA} = \tilde{\Delta}_{\omega} F_{KH}(\langle \mathrm{VTM} \rangle). \tag{46}$$

Here the subscript SLA stands for Shear Layer Adapted, $\langle \mathrm{VTM} \rangle$ denotes the average of the VTM quantity over neighboring cells, which is needed to eliminate strong downward excursions experienced by the local values of VTM in the developed turbulence flow regions, and the function F_{KH} is aimed at unlocking Kelvin-Helmholtz instability in the initial part of shear layers.

To achieve this, the function should be designed so that it remains small at the $\langle \mathrm{VTM} \rangle$ values less than some prescribed threshold value and then rapidly increases up to 1.0 with the $\langle \mathrm{VTM} \rangle$ increase. One possible type of such a function is a simple piecewise-linear function defined as:

$$F_{KH}(\langle \mathrm{VTM} \rangle) = \max\left\{ F_{KH}^{min}, \min\left\{ F_{KH}^{max}, F_{KH}^{min} + \frac{F_{KH}^{max} - F_{KH}^{min}}{a_2 - a_1}(\langle \mathrm{VTM} \rangle - a_1) \right\} \right\} \tag{47}$$

Here $F_{KH}^{max} = 1.0$ and F_{KH}^{min}, a_1 and a_2 are adjustable empirical parameters which were set equal to 0.1, 0.15, and 0.3 respectively.

Considering that in the inviscid flow regions the quantity $\langle \mathrm{VTM} \rangle$ strongly oscillates in space, in order to avoid possible numerical issues this may cause, the definition of VTM (Chauvet et al. 2007) is further modified as follows:

$$\mathrm{VTM} \equiv \frac{\sqrt{6}\left|\left(\hat{\mathbf{S}} \cdot \boldsymbol{\omega}\right) \times \boldsymbol{\omega}\right|}{\boldsymbol{\omega}^2 \sqrt{3tr\left(\hat{\mathbf{S}}^2\right) - \left[tr\left(\hat{\mathbf{S}}\right)\right]^2}} \max\left\{1, \frac{0.2\nu}{\max\left\{\left(\nu_t - \nu_{t,\infty}\right) 10^{-6} \nu_{t,\infty}\right\}}\right\} \tag{48}$$

which results in large values of *VTM* in the inviscid flow region and, therefore, deactivation of the F_{KH}, (at large values of *VTM*, $F_{KH}(\langle \mathrm{VTM} \rangle) = 1.0$).

Finally, in the DDES approach the F_{KH} function (1) has to be deactivated also in attached boundary layers, where DDES should work in RANS mode. So, for the wall-bounded flows the function is further modified as follows Shur et al. (2015):

$$F_{KH}^{\lim} = \begin{cases} 1.0, \; if \; f_d < (1 - \varepsilon) \\ F_{KH}, \; if \; f_d \geq (1 - \varepsilon) \end{cases} \tag{49}$$

where f_d is the delay function of DDES (Spalart et al. 2006) and ε is an empirical constant.

Based on the numerical experiments carried out in Shur et al. (2015) for the zero pressure gradient boundary layer, this constant was set equal to 0.01.

Thus, a final relation for the proposed length-scale reads as:

$$\Delta_{SLA} = \tilde{\Delta}_{\omega} F_{KH}^{\lim} \left(< \text{VTM} > \max \left\{ 1, \frac{0.2v}{\max\left\{ (v_t - v_{t,\infty}), 10^{-6} v_{t,\infty} \right\}} \right\} \right) \tag{50}$$

Results of simulations illustrating a high efficiency of the thus modified subgrid length-scale within SA DDES of the spatially evolving plane shear layer (test case F.2), wall-mounted 2D hump (test case I.4), and round jet (test case I.5), and are presented in Part III (Chapter "Free Shear Layer"), Part IV (Chapter "2D Wall-Mounted Hump") and Part IV (Chapter "Single-stream Round Jet at M = 0.9"), respectively.

Springer

http://www.springer.com/978-3-319-52994-3

Go4Hybrid: Grey Area Mitigation for Hybrid RANS-LES Methods
Results of the 7th Framework Research Project Go4Hybrid, Funded by the European Union, 2013-2015
Mockett, C.; Haase, W.; Schwamborn, D. (Eds.)

2018, XII, 280 p. 172 illus., 155 illus. in color.,
Hardcover
ISBN: 978-3-319-52994-3